MODUS QA

Measuring Geometric Distortion with Sub-Millimeter Accuracy in MRgRT QA:

A Lighter, Faster, Single Acquisition, Large Field-Of-View Full 3D Approach with Simple Workflow Using the Harmonic Analysis Method

WHITE PAPER

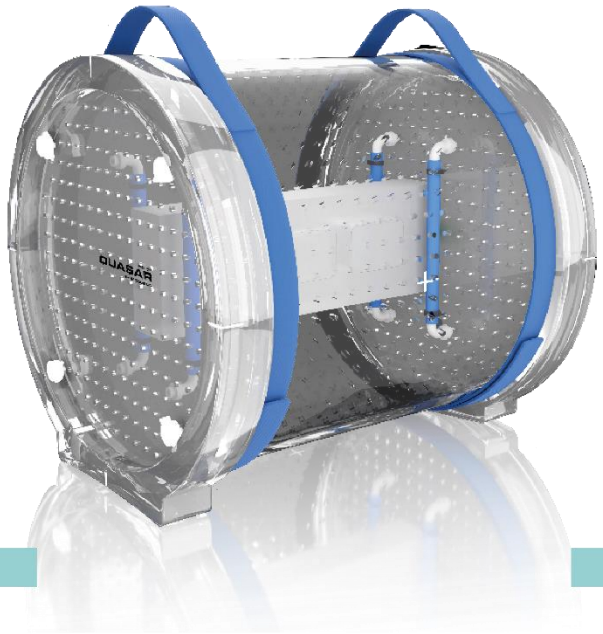

Executive Summary

The use of Magnetic Resonance Imaging (MRI) for guidance has expanded from research to clinical applications in the past decade. While MRI has many advantages related to image quality, image geometric distortion due to vendor design trade-offs and limitations dictated by cost and patient considerations require QA tools to ensure distortion is measured and acceptable limits are achieved to ensure accuracy of treatment. Advanced and demanding applications (Diffusion Weighted Imaging, Head and Neck Stereotactic Radiosurgery, MRI Guided Neurosurgery) require sub-millimeter accuracy. The factors which affect MRI Geometric Image Distortion are reviewed, as well as the tools that can be used to quantify distortion. A recommended method for measuring a full 3D distortion vector field using a lighter weight, large field of view hollow boundary phantom utilizing the harmonic analysis approach to achieve sub-millimeter accuracy (error < 0.1mm) is presented.

Legal & Copyright Notice

Table of Contents

1. Introduction

Over the last decade, Magnetic Resonance Guided Radiation Therapy (MRgRT) has received considerable and increasing interest in the Cancer Research and Clinical Treatment community for several compelling reasons:

1. The utility of Magnetic Resonance Imaging (MRI) for high contrast patient, tumor, and organ registration with no additional ionizing radiation from the imaging modality.

2. The ability to provide real time motion tracking of moving tumors with exquisite soft tissue contrast to see what is being treated, which eliminates the need for an Internal Target Volume (ITV) around the Clinical Target Volume (CTV) on moving targets and thus reduces the Planned Treatment Volume (PTV) margins with gating and breath hold techniques, with no additional ionizing radiation from the imaging modality.

3. The ability to treat challenging cancers more effectively, such as pancreatic, liver and lung cancer, that cannot be easily treated on regular Linacs.

4. The potential to provide adaptive beam tracking and advanced motion correction to eliminate the need for breath holding, gating, or patient immobilization while increasing therapeutic target dose and reducing toxic dose to adjacent Organs-at-Risk and healthy tissue, as well as reducing the overall number of fractions and patient visits required, leading to better outcomes and higher quality of life for patients after treatment.

5. The potential to implement advanced diagnostic and cancer staging functional imaging sequences and contrast mechanisms such as Diffusion Weighted Imaging (DWI) and Amide Proton Transfer (APT) for improved cancer detection, treatment, and treatment response.

The use of MRI for Guided Therapy places an increased demand on spatial or geometric accuracy not normally associated with Diagnostic Applications, where contrast is more important than spatial accuracy. Diagnostic MRI system manufacturers historically provide acceptance and commissioning testing specifications over a 20 cm Diameter Spherical Volume (DSV), whereas MR SIM and MR-Linac manufacturers now also include an expanded 34 cm DSV specification to include the entire Treatment and Planning Volume. This effectively places an increased demand for MR SIM and MR-Linac manufacturers to maintain spatial accuracy to much larger volumes than previously required for Diagnostic MRI applications.

A review of the factors which affect MRI spatial accuracy, and what can be done to manage and measure it, follows.

2. Technical Background

2.1. Formation of Magnetic Resonance Signal

Unlike X-Ray, CT (kV or MV), Ultrasound, PET, SPECT and other related imaging modalities, MRI does not use projection, reflection, emission, or refraction mechanisms found in optical imaging methods, where acceptable spatial accuracy is normally assumed. MRI relies on a technique that exploits the interaction of three distinct non-ionizing static and time varying magnetic fields with atomic elements found within the body, with spatial accuracy directly related to magnetic field amplitude and phase accuracy.

The first magnetic field B_0 is the main magnetic field, identified by the Field Strength (measured in Tesla, T) associated with the MRI system (0.35 T, 1.5 T, 3.0 T (2.9 T - Siemens/Canon), 7.0 T *etc.*). This powerful magnetic field is chosen based on its ability to affect, on a fundamental quantum mechanical level, the intrinsic net magnetic moment due to the angular momentum (or spin) of any atom with an odd number of protons and/or neutrons; chiefly hydrogen (^{1}H) is used in MR Imaging and Spectroscopy but other nuclei, such as ^{31}P, ^{23}Na, ^{7}Li, ^{13}C, ^{19}F can also be detected for metabolic studies. When a material in liquid or semi-solid state, abundant in such atoms (such as water ($^{1}H_2O$) in soft tissues or fat (^{1}H-C...) in adipose tissue) is placed in a sufficiently powerful magnetic field, a small percentage of the spinning nuclei will align in the direction of the main magnetic field. It is this alignment, or interaction, which fundamentally enables MRI. Solid materials provide very weak MRI signal because atomic motion is heavily constrained.

The interaction of the nuclear spin and its associated resonance frequency is directly proportional to the Field Strength, according to Larmor's equation:

$$f = \gamma B_0 / 2\pi$$

Where: f is the resonance frequency, γ is the "Gyromagnetic Ratio", unique for each chemical compound while the resonance frequency is also known as the "Larmor frequency"

Generally, at higher field strengths, the MR signal increases but so do various image artifacts such as chemical shift and susceptibility distortion. The main magnetic field is typically produced by a superconducting solenoid coil (array of conducting loops) in a large metal cryostat with a patient aperture and is typically a horizontal bore on most clinical MRI systems. MRI forms images based on the interaction of the B_0 field

with ^{1}H, which is present in both water (H_2O) and adipose tissue (containing H-C chains), both of which are abundant in human subjects.

The second magnetic field B_1 (or B_{RF}) is a pulsed (limited time duration) time-varying magnetic field that corresponds to the Larmor Resonance Frequency, and falls in the Radio Frequency (RF) spectrum (13 MHz to 300 MHz) for Field Strengths between 0.35 T to 7 T. The B_1 field is associated with RF coils, RF coil arrays, and the integrated RF Body Coil normally found in clinical MRI scanners which produce a primarily near-field magnetic field (within one wavelength of the radiating source). The B_1 field is applied orthogonally to the static B_0 field as a pulsed RF magnetic field that knocks the ^{1}H spinning nuclei temporarily out of alignment with the B_0 field. When the B_1 field ceases, the bulk net magnetic moment of the ^{1}H spinning nuclei undergo a realignment process (precession), like a spinning top, and return to their low energy state, aligning back with the B_0 field. This produces an RF signal known as the Free Induction Decay signal which forms the basis of the MR signal, also detected by the B_1 RF coil.

The third magnetic field B_G is formed by a series of three orthogonal gradient coils which correspond to the X, Y and Z cardinal axes associated with DICOM images. The three X, Y and Z gradient coils apply a pulsed magnetic field gradient in the Audio Frequency range (hence the knocking noises of MRI) that adds to or subtracts from the B_0 field as a function of X, Y, and Z position, providing variations in the phase, frequency, and slice selection of the ^{1}H spinning nuclei, and hence spatial encoding to form the MR Image in 2D and 3D (this 1973 idea led to Lauterbur and Mansfield winning the Nobel Prize in Medicine 2003!).

It is the first and third set of the three magnetic fields (Main and Gradient) which primarily determine the frequency (and phase) of the ^{1}H spinning nuclei and hence their representative spatial image position and the geometrical accuracy of the resulting image. This begs the question: What happens when the applied B_0 and B_G fields are not what we expect?

2.2. Gradient Non-Linearities (GNL) – distortion in B_G

All MR manufacturers design gradient coils with some design trade-offs and limitations dictated by cost and patient considerations. It is not practical to design MR systems sufficiently long with small enough bores to ensure gradient coils are optimized without software correction, as this would lead to excessively heavy, costly, and small-bore systems that trade off key requirements (lower weight, lower cost, patient friendly, wide-bore systems) for gradient performance. Practical design considerations and required trade-offs will lead to Gradient Non-Linearity with increased distance from isocenter.

- MRI is based on assumption of linear encoding of position to frequency over FOV…
  with some design trade-offs
- Linearity is high near gradient coil isocenter but falls off with increasing distance

- Main effects:
  - Anatomical compression (S-I)
  - Anatomical dilation (A-P, R-L)
  - Aliasing

- Field strength, sequence independent

- Arises from vendors being forced to trade-off linearity for performance: shorter bore lengths (reduce claustrophobia) and larger bore diameter (to accommodate obesity)

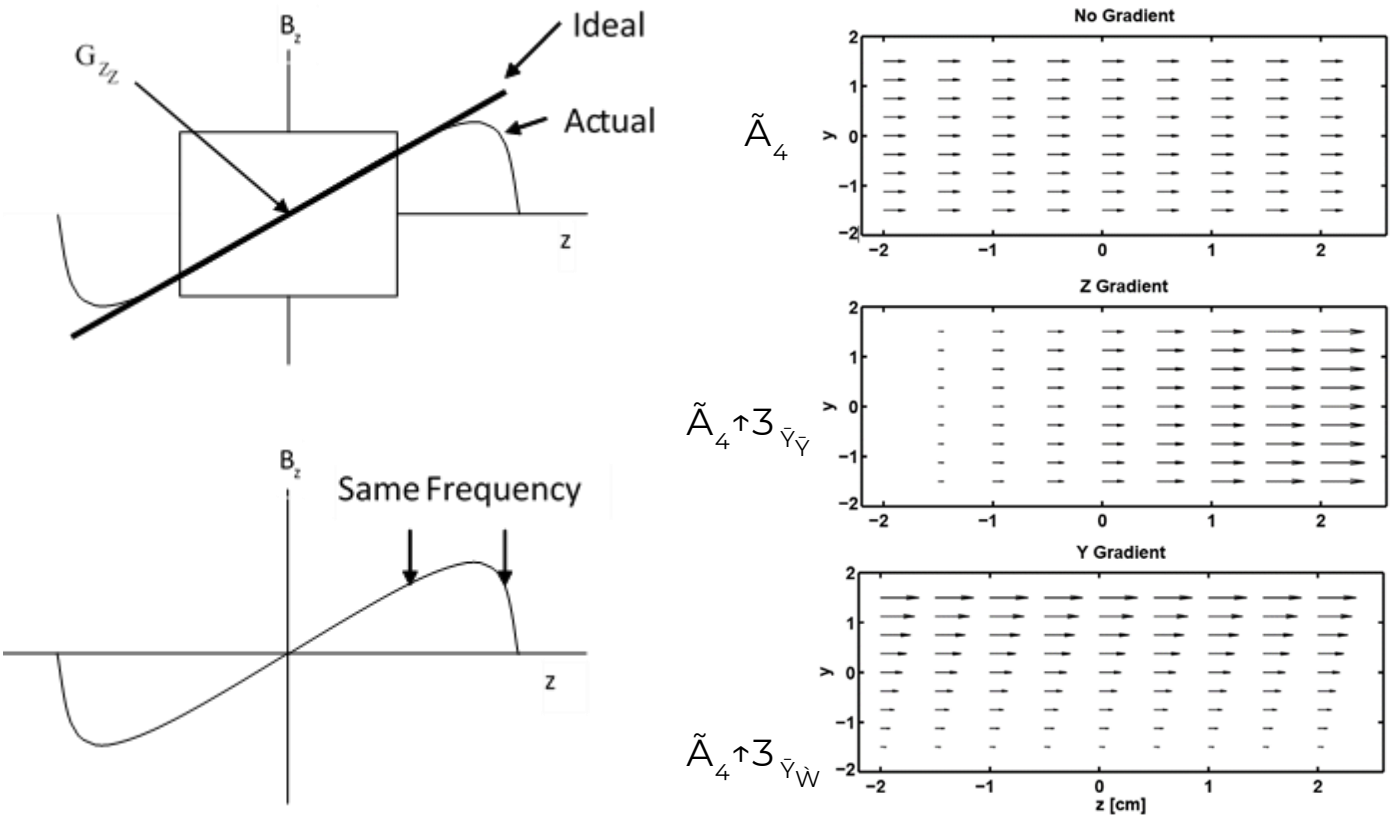

Figure 1. Gradient coil non-linearities are caused by design trade-offs to address economic concerns and patient requirements

2.3. Vendor Corrections to Gradient Non-Linearities – Post-Processing

All MRI vendors employ software correction of Gradient Coil Non-Linearity in 2D and 3D imaging, and apply the correction based on harmonic analysis of the uncorrected fields to produce a 2D and 3D distortion corrected image suitable for Diagnostic and Guided Treatment applications. Gradient coil designers use harmonic analysis methods, among other field target techniques, to design gradient coils. The gradient coil winding locations and patterns are optimized to satisfy boundary conditions which attempt to produce a 3D linear gradient field over an acceptable Field of View (FOV), with design limitations as noted. The requirement for large diameter, short length MR bores confounds perfect gradient linearity, necessitating the use of Spherical Harmonic based 2D and 3D image correction to Gradient Non-Linearities for all MR manufacturers.

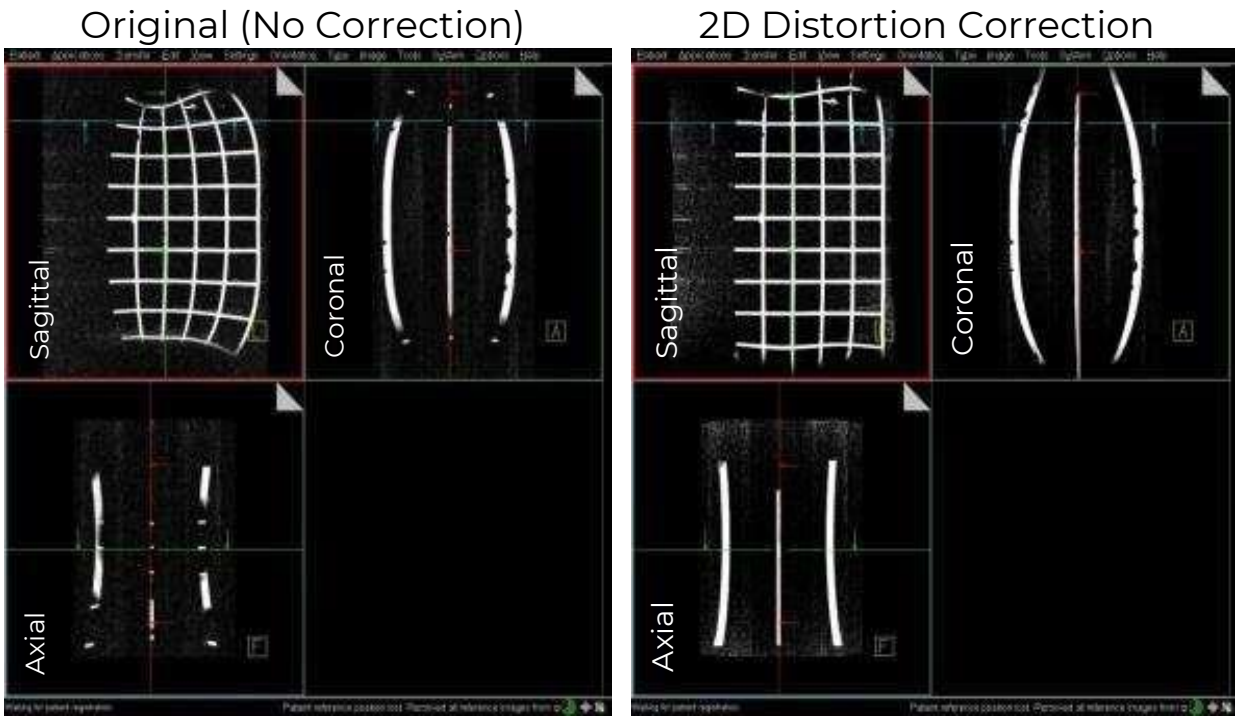

Conventional grid phantom with no correction

Corrects “in-plane” distortion only
Other planes not corrected

Figure 2. Gradient Coil Non-Linearities without correction, and with 2D and 3D correction applied

3D Distortion Correction

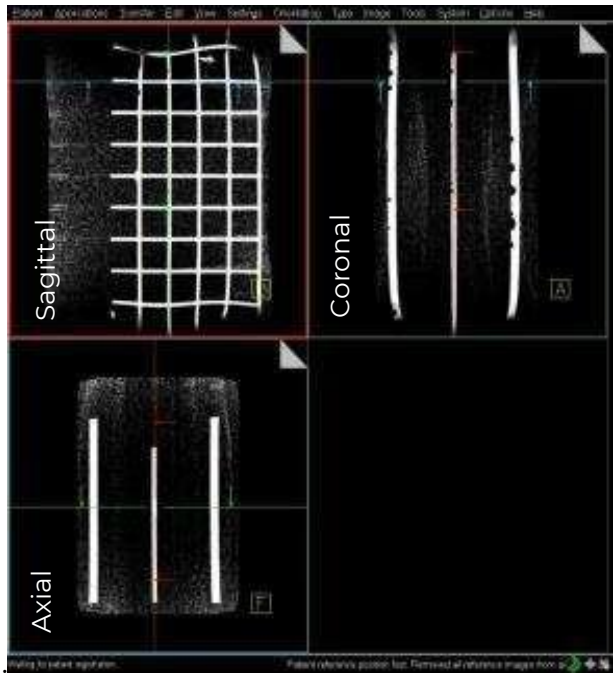

Corrects distortion in all three planes:
Required for radiation treatment planning
Can run automatically during reconstruction

Figure 2 Cont'd. Gradient Coil Non-Linearities without correction, and with 2D and 3D correction applied

All MR vendors utilize spherical harmonics to correct for Gradient Non-Linearity and B_0 inhomogeneity, with modern MR SIM systems and MR Linacs designed for 35 cm FOV treatment volumes.

2.4. Main Field B_0 Homogeneity: Subject/Object Induced Distortion and Vendor Shimming

All main field magnets for MRI generate strong B_0 magnetic fields which are designed to be homogeneous or of uniform intensity over a large volume. The typical size of the imaging volume is a 350 mm to 500 mm Diameter Spherical Volume (DSV), over which the field intensity variations (ΔB_0 inhomogeneity - which lead to image distortion ΔF) are within an acceptable Diagnostic Imaging range (<5 mm image distortion). It is noted that one MRI manufacturer has implemented a magnet design which optimizes the homogeneity over a cylindrical volume, in contrast to the conventional spherical or ellipsoidal volume.

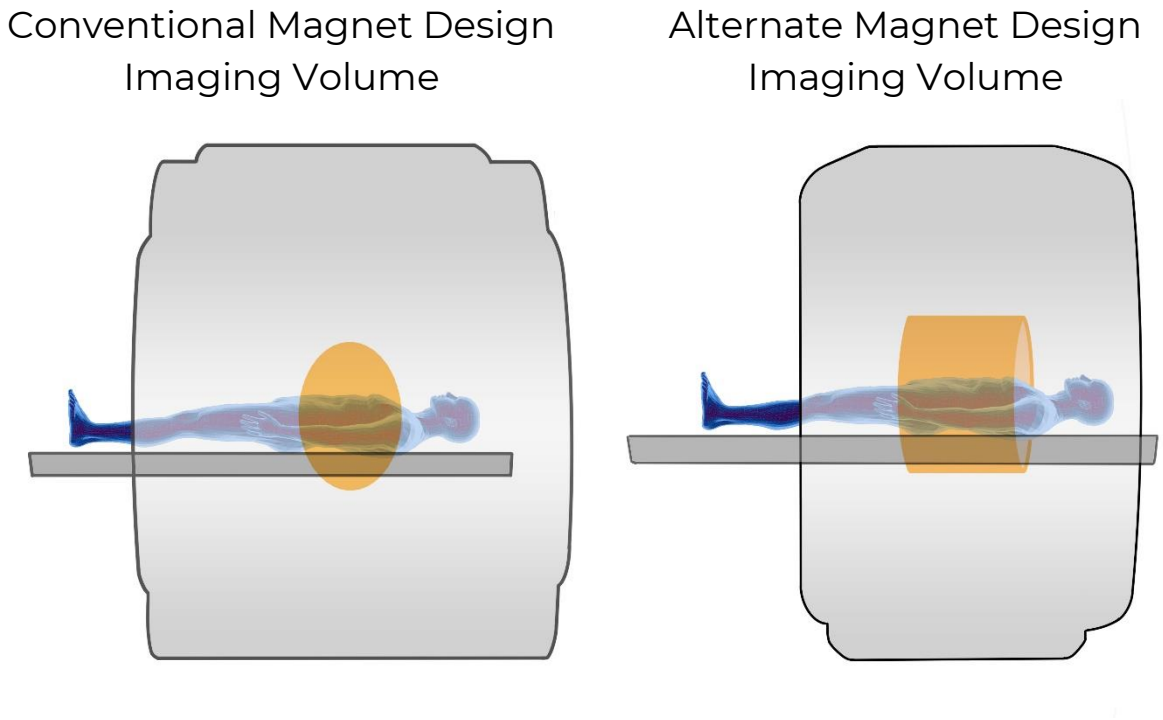

Figure 4. Representative Homogeneous Imaging Volumes for Conventional and Alternative Magnet and Gradient Designs

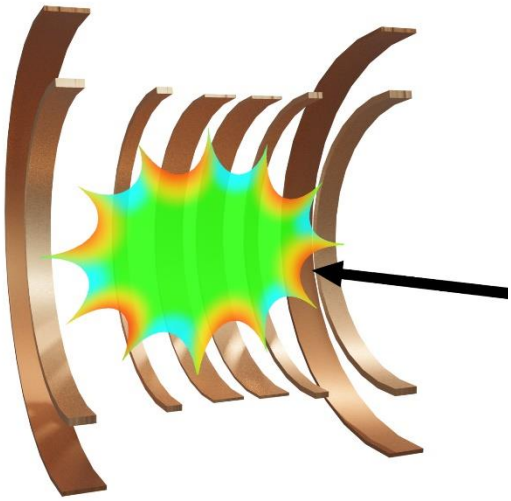

Inhomogeneous regions at the edge of all manufacturers specified imaging volumes can be significant and may exceed acceptable distortion for precision MR Guided RT (<< 2mm of image distortion is required).

Modern actively shielded high-field MRI magnet: coils and high uniformity central B_0 field

Figure 5. Main Field B_0 Homogeneity on a Modern MR SIM System

When a human subject or phantom is placed in the bore of an MRI system, the magnetic susceptibility of the object will lead to undesirable perturbations of the B_0 field (Stanescu *et al.*, 2012; Tijssen *et al.*, 2019). Vendors employ proprietary dynamic harmonic analysis shimming techniques to improve the B_0 homogeneity. However, the larger perturbations at the interfaces between air and signal producing material cannot be corrected by shimming. Such examples include nasal/ear/throat canals in human subjects and phantom air/acrylic singularity interfaces. Advanced tools are required to correct for this, and methods for correcting object induced susceptibility distortion will be later described. Chemical shift in the frequency encode direction is noted between water and hydrocarbon rich tissue, which can be minimized with higher bandwidths and/or fat/water suppression techniques.

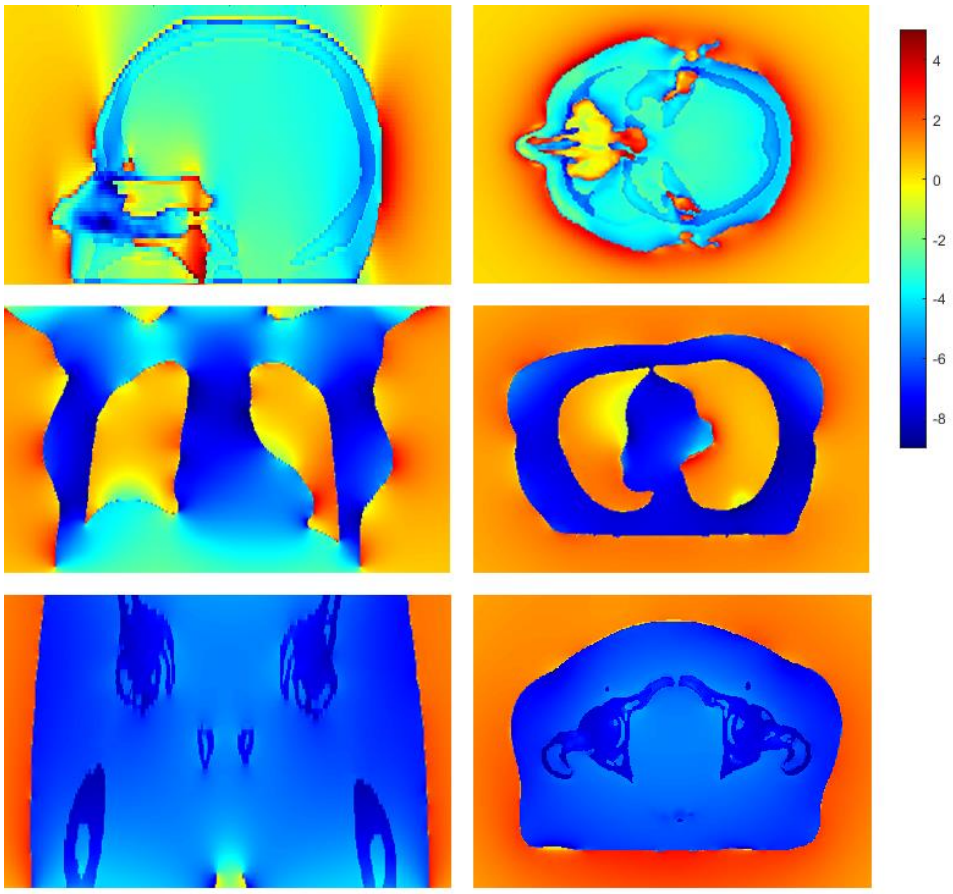

Figure 6. Susceptibility-induced B_0 perturbation maps for two MR-Linac system configurations in the case of a typical brain patient anatomy. Column (a) displays the simulation results for B_0 along z-axis for the bore-type magnet, and column (b) shows the results for the biplanar magnet configuration with B_0 along y-axis [in the (x, y)-plane]. Phantoms cannot adequately represent patient distortion.

2.5. Summary: Three Main Sources of Geometric Distortion in MRI

Gradient Non-Linearity is caused by considerations related to the cost of MRI equipment and the wellbeing of patients; it is recognized as a source of distortion across all vendors, regardless of field strength. B_0 inhomogeneity distortion is correlated to MR bore size constraints, which limit the 3D volume over which an acceptable FOV can be maintained for precision MRgRT applications; typically, no greater than a 35 cm DSV is used in MR-guided Linacs. Lastly, the object susceptibility distortion due to the imaged object (human subject or phantom) is reduced but not fully eliminated by vendor shimming algorithms.

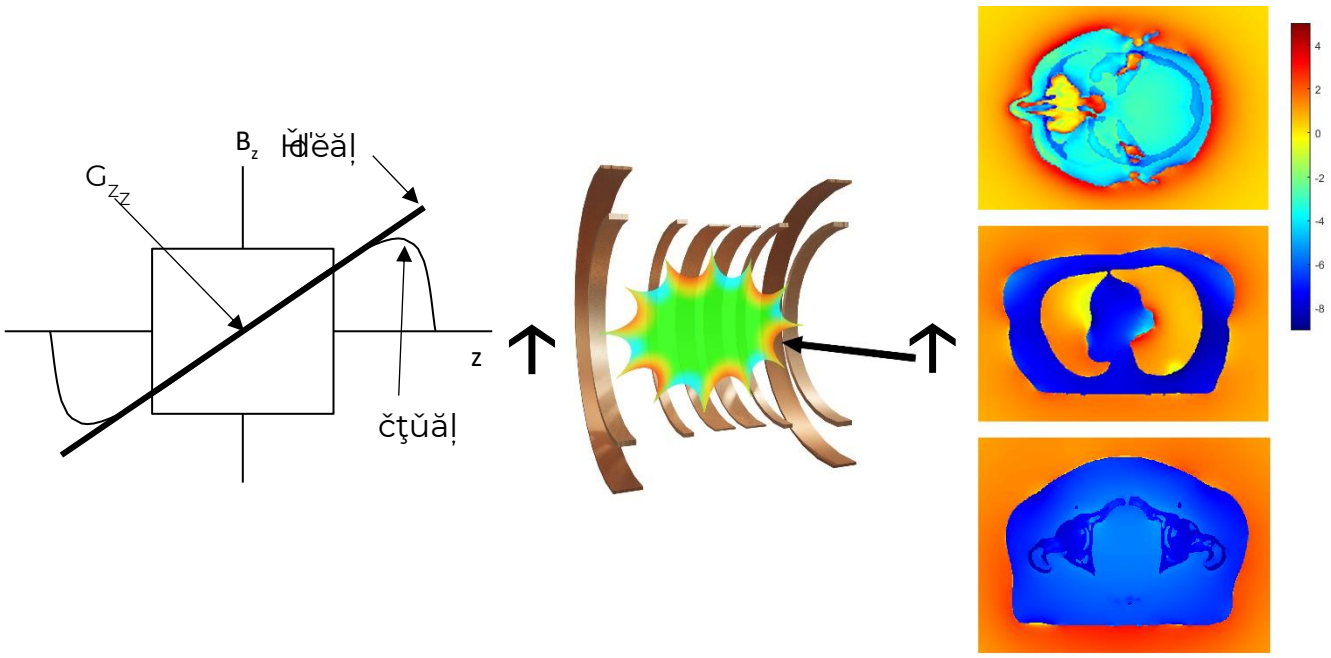

Gradient Non-Linearity	B_0 Inhomogeneity	Patient Susceptibility Induced Changes to B_0
Field strength, sequence independent	Field strength, frequency encode direction, BW, sequence dependent	

Figure 7. Three Main Sources* of Distortion in MRI

*A fourth source of distortion not illustrated arises from the gradient coil pulsed magnetic fields external to the gradient coils. In modern MRI systems, an active shield coil compresses the external gradient magnetic fields between the gradient coil windings and the surrounding active shield coil so that only insignificant residual eddy currents are induced in the stainless-steel magnet cryostat bore. For some advanced demanding sequences (EPI, DWI), the residual gradient eddy currents may lead to transient geometric distortion and image artifacts.

2.6. Effect of Gradient Field Strength on B_0 and Object Susceptibility Distortion

One of the simplest ways to manage geometric distortion arising from B_0 Inhomogeneity and Object Susceptibility induced changes to B_0 is to increase the gradient strength or bandwidth which reduces the relative contribution to total distortion. In the example below, a B_0 perturbation equivalent to 500 Hz in the frequency encode direction is experienced. Scanning at 100 Hz/Pixel and 1000 Hz/Pixel bandwidths is compared showing B_0 perturbation related distortion is reduced from 5 pixels to 0.5 pixels. Recommendations for MRgRT scanning are bandwidth minimums of 100 Hz/Pixel at 0.35T, 300 Hz/Pixel at 1.5T and 600 Hz/Pixel at 3T.

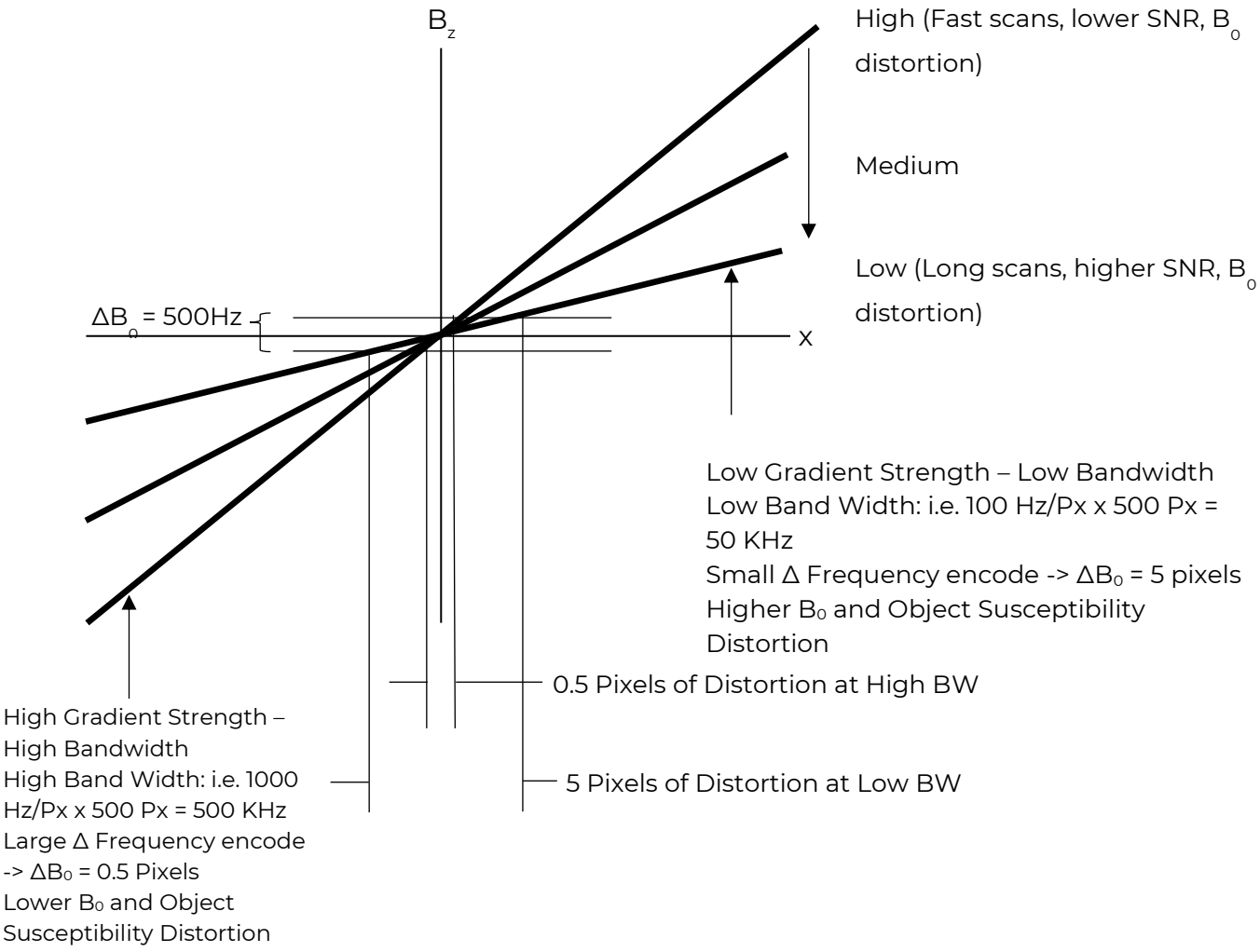

Figure 8. Effect of Bandwidth on Distortion in MRI

3. Recommendations for measuring geometric distortion in MRI

3.1. Is There a Way to Measure MR System B_0 Inhomogeneity Distortion and GNL Distortion Separately?

As noted by (Baldwin *et al.*, 2007), scanning an object twice with opposing polarity in the frequency encode direction permits the separation of B_0 and Gradient Non-Linearity (GNL) distortion, since the B_0 distortion is sensitive, while GNL distortion is insensitive, to the gradient polarity. Therefore, acquiring two scans of an object and performing a scalar mathematical operation permits separating B_0 and GNL distortions. A representative example will be shown later.

3.2. What Recommended Methods are Available to Measure MRI Geometric Distortion?

Several standards bodies and professional medical/scientific societies (NEMA-MITA, IEC, AAPM, ACR) have recommendations on methods of measuring Image Quality parameters, with specific guidelines related to measuring 2D and 3D geometric distortion.

Historically, recommendations have been biased towards 2D applications for Diagnostic Radiology with testing specifications defined over a conservative 20 cm Diameter Spherical Volume (DSV).

1. Small Phantom Test Guidance for the ACR MRI Accreditation, American College of Radiology, 2018
2. Phantom Test Guidance for the ACR MRI Accreditation Program, American College of Radiology, 2018
3. Quality Assurance Methods and Phantoms for Magnetic Resonance Imaging, AAPM Report No.28, 1990

Recently, national, and international standards have been updated to address the growing use and application of MRI for advanced 3D guided applications with larger 34 cm DSV specification volumes appropriate for MR SIM and MR-Linac QA:

4. National Electrical Manufacturers Association - Medical Imaging Technology Alliance - NEMA MITA MS-12 2016 - *Quantification and Mapping of Geometric Distortion for Special Applications*
5. International Electrotechnical Commission - IEC 62464-1 2018 *MAGNETIC RESONANCE EQUIPMENT FOR MEDICAL IMAGING – Part 1: Determination of essential image quality parameters.*

Grid phantoms (large and heavy or small and light), fiducial array phantoms, and modern hollow boundary phantoms based on the use of harmonic analysis, as described in the last two aforementioned standards, are all tools available to the practitioner interested in implementing MRI geometric distortion Quality Assurance (QA) methods for commissioning, acceptance testing, and periodic QA of MR SIM and MR-Linac systems. With the advent of MR guidance in applications *demanding sub-millimeter accuracy and precision*, measurement, and management of residual distortion, even after 3D vendor distortion correction is applied may be of concern. Such applications include head and neck Stereotactic Radiosurgery (SRS), Stereotactic Ablative Radiotherapy (SABR) of the pancreas, MR guided Neurosurgery and improved DWI-ADC calibration correcting for residual GNL post-vendor correction errors.

A summary of the recent NEMA-MITA and IEC recommendations for good design practice which maximize clinical workflow and minimize sources of error for geometric distortion phantoms to achieve sub-millimeter accuracy and precision are now presented. These are based on empirical data gathered by Modus QA with Hollow Boundary (Modus QA MRID$^{3D™}$), Solid Acrylic Spherical Lebedev Quadrature Boundary (Modus QA W-I-P) and Positive Channel Solid Acrylic Cuboid Grid (Modus QA GRID$^{3D™}$) geometric distortion phantoms at 0.35 T, 1.5 T, 3.0 T, and 7.0 T.

3.3. Common MR/CT Phantom Materials – Thermal Properties

Acrylic and other plastics are commonly used to form liquid containing phantoms with fiducial arrays or grids at known locations to ascertain geometric fidelity in MRI. Aqueous solutions with a contrast agent may be used to provide an appropriately physiological T1 and T2 value for the contrast media at lower field strengths up to 1.5 T. At 3.0 T and higher field strengths the use of either mineral oil or silicone oil is preferred, as both have much lower dielectric constant than water which helps to mitigate the dielectric resonance effect. Note that mineral oil has an inherently physiological T1 and T2 (300 ms and 60 ms respectively at 1.5 T) while silicone oil requires the use of complex processes to modify the T1/T2 (dependent on viscosity) with expensive chelated gadolinium complexes.

In the case of using poly(acrylamide) (PMMA or acrylic) as the plastic material for the phantom structure, it is instructive to consider the volumetric coefficient of thermal expansion of readily available liquid contrast media (water and mineral oil) and PMMA:

Volumetric coefficient of thermal expansion:

$$\alpha_{PMMA} = 72 \times 10^{-6}\ °C^{-1}$$
$$\alpha_{Water} = 214 \times 10^{-6}\ °C^{-1} \text{ -> } 3 \times \text{PMMA}$$
$$\alpha_{Mineral\ Oil} = 764 \times 10^{-6}\ °C^{-1} \text{ -> } 10 \times \text{PMMA}$$

Empirical data measuring the pressure change (ΔP) due to thermal expansion of a liquid fully filling a rigid solid enclosure (such as any uncompensated liquid filled MRI Geometric Distortion Phantom) yields the following results:

ΔP per °C of change in temperature: Mineral Oil ΔP= 13.75 kPa/°C = 2psi/°C, Water ΔP= 8.3 kPa/°C = 0.6 psi/°C

From the above, it can be seen that there is a significant increase in internal phantom pressure associated with a rise in temperature above nominal filling or room temperature due to the much greater volume coefficient of thermal expansion of liquids relative to plastics, such as PMMA. Subjecting the phantom to environmental temperature cycling in shipping and using the phantom in the clinic yields the following empirical results:

Shipping filled phantoms in warm climates: ΔT = +20°C -> ΔP ~ 0.3 MPa (40 psi) for mineral oil, 0.1 MPa (14 psi) for water.

Temperature change in the clinic: ΔT > +5°C -> ΔP ~ 0.075 MPa (10 psi) for mineral oil, 0.025 MPa (3.5 psi) for water.

The resulting internal pressure build up is sufficient to cause deformation of the phantom walls, inducing geometric distortion of the phantom and is identified as a source of error. This source of error can be mitigated through the use of pressure compensating expansion reservoirs designed into the phantom, as per NEMA-MITA MS-12 2016 and IEC 62464-1 2018 recommendations and Modus QA patents US10,180,484 (2017) and US10,310,048B2 (2019). The expansion reservoirs function to maintain low pressure within the phantom and divert thermally induced liquid expansion to a flexible elastomer reservoir/chamber while stabilizing the critical plastic structures and fiducial positions, maintaining critical geometric stability of the phantom.

3.4. Common MR/CT Phantom Materials – Susceptibility Properties

The volume magnetic susceptibility of common MR/CT phantom materials, as noted by (Schenck, 1996), are:

Volume Magnetic Susceptibility of Common MR/CT Phantom Materials at 20°C:

PMMA: χ_V = -9.01 ppm
Water: χ_V = -9.03 ppm
Mineral oil: χ_V = -9.24
Air: χ_V = -0.31 ppm

Note that PMMA, water and mineral oil have a relatively good susceptibility match. The induced susceptibility gradient distortion due to the difference between acrylic and mineral oil has been calculated at clinical bandwidths as below 0.15mm at 1.5 T in (Baldwin *et al.*, 2007). Empirical phantom imaging and geometric distortion analysis by Modus QA indicates that when the separation between air and liquid contrast media, formed by the acrylic walls and boundaries of the phantom, is less than 6mm noticeable susceptibility distortion at the air/plastic/liquid MR contrast media interface is apparent (> 0.5 mm at low bandwidths at 1.5 T for a 1.5mm separation).

As noted previously, when an object (human subject or phantom) is placed in an MR scanner, the inherent magnetic properties of the object will interact with the B_0 field: a highly homogeneous B_0 field can be achieved in an empty, air filled bore of uniform susceptibility, but once an object is placed in the bore, the magnetic susceptibility of the object will induce a susceptibility gradient with surrounding air at the air/object boundary, as well as between materials of different susceptibility within the object (Wapler *et al.*, 2014).

Modern shimming of the B_0 field to globally improve the homogeneity involves the use of dynamic harmonic analysis and does result in lower overall distortion but cannot correct for local perturbations with extrema in gradients (air filled nasal/ear/throat cavities or air/thin plastic/liquid MR contrast media interfaces). Therefore, patient-specific B_0 maps are acquired and employed by advanced centers to correct for unique patient-induced susceptibility distortion (Stanescu *et al.*, 2012; Tijssen *et al.*, 2019).

Phantom Finite Element Modeling can be used to assign susceptibility to air, plastic, and MR liquid contrast media for physics and engineering-based CAD models in analysis software. Corrections to phantom susceptibility geometric distortion can be developed and implemented to consider field strength, bandwidth and frequency encode direction, followed by validation with testing at different field strengths.

3.5. Common MR Phantom Liquid Contrast Media Properties - Empirical Observations

Aqueous solutions with various contrast agents ($MnCl_2$, $CuSO_4$, $NiCl_2$, gadolinium complexes *etc.*) are commonly used as convenient or accessible MRI contrast media. With the advent of higher field strengths and a requirement for higher geometric precision, alternatives to aqueous solutions and their negative attributes described below are recommended:

Water: *Caveats*

- Is absorbed by acrylic/plastics and changes structural dimensions – a source of error
- Absorbs gas and may release dissolved air as bubbles over time
- Can freeze during shipping in winter and expand, causing deformation and or damage to phantom
- Has a high dielectric constant: ~80, leading to signal intensity inhomogeneity above 1.5 T
- Must be doped ($MnCl_2$, $CuSO_4$, $NiCl_2$, Gd complexes) to obtain physiological T1, T2
- Preservatives required to avoid biological fouling over time

Silicone Oil: *Caveats*

- Must be doped with heat processed chelated Gd complexes to obtain physiological T1, T2
- Contrast agent subject to falling out of suspension with cold temperature cycling
- Expensive and limited in supply due to high worldwide demand and few suppliers
- Requires advanced methods for handling and clean-up, few safe solvents readily available

Mineral Oil: *Recommended (Gach, 2020; Modus QA Empirical Data)*

- *Not absorbed by acrylic and does not change dimensions of acrylic/plastic structures*
- Keeps dissolved gasses in solution
- Low freezing point (-40 °C/ °F)
- *Low dielectric constant: ~3 -> signal uniformity at 3 T/7 T*

- Physiological T1, high contrast T1w imaging, fast Gradient Echo scanning (TR, TE < 10 mS)
- Does not suffer biological fouling

3.6. Other Factors Related to Geometry

NEMA-MITA MS-12 2016 and IEC 62464-1 2018 recommend manufacturing tolerances for geometric distortion phantoms of 10% of the imaging resolution for 2D and 3D phantoms, which translates to a 0.1 mm manufacturing tolerance for 1mm resolution imaging QA associated with MR SIM and MR-Linacs.

3.7. Automated Control Point Finding Software

NEMA-MITA MS-12 2016 and IEC 62464-1 2018 recommend the use of automated control point finding software to remove inter- and intra-observer variance as a source of error. The use of highly refined and robust algorithms (with advanced image processing and heuristics) to work with phantom design elements is recommended to help identify and correct for phantom misalignment and patient table roll-pitch-yaw. Otherwise, such effects may be misinterpreted as distortions and become a source of error associated with the phantom positioning rather than the MRI system itself. Additionally, contrastive or distinguished landmark fiducials may be used for registering key reference point locations on the phantom to ensure correct automated software detection under cases of high distortion (e.g., vendor GNL distortion correction turned off with low bandwidths).

4. Proposed solution to the problem: The Harmonic Analysis Advantage

Our solution is a commercially available geometric distortion phantom that minimizes all sources of error to achieve sub-millimeter accuracy with improved workflow and is amenable for site-to-site shipping and comparisons.

A novel, modern geometric distortion phantom, based on the use of well-established harmonic analysis techniques currently used for MRI gradient coil design, GNL distortion correction, and B_0 shimming, has recently been adapted for sparse and highly efficient sampling and measurement of inherent MRI B_0 and GNL system distortion (Tadic *et al.*, 2014):

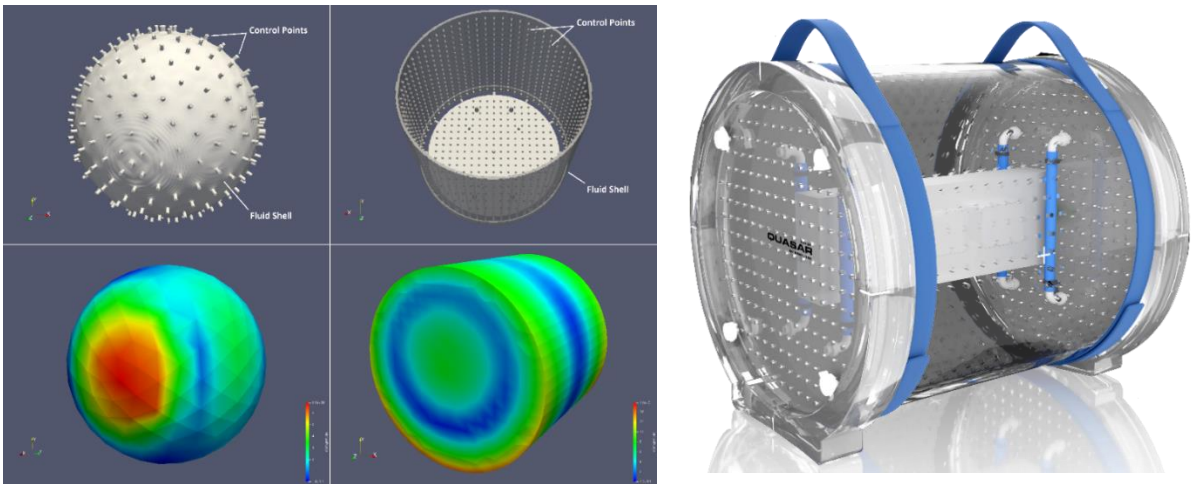

Figure 9. Closed hollow boundary shapes amenable to the Harmonic Analysis Method for measuring MRI Distortion

The harmonic analysis method is a fundamental analytical tool for well-defined boundary value problems in electromagnetics (including MRI) and other fields of science and engineering (fluid flow, gravity, thermodynamics etc.). In short, the measured boundary condition on an enclosed hollow volume (sphere, cylinder, etc.), if sufficiently sampled, completely defines the conditions within the enclosed volume. Reduced to practice on an MRI geometric distortion phantom, this permits the use of a hollow, lighter phantom with a sufficient number (slightly over-sampled) of MRI signal producing fiducials uniformly distributed around the boundary of the phantom. The measurement of distortion around the boundary of the phantom is sufficient to derive the entire 3D geometric distortion deviation vector field (DVF) within the enclosed volume using harmonic analysis. Not only does this result in a lighter phantom compared to conventional grid phantoms, it also greatly reduces the number of detected fiducials required to measure MRI geometric distortion over large 35 cm Fields of View typical of MRgRT. As an example, the Modus QA MRID^{3D} phantom contains just over 1500 fiducials to calculate distortion at over 11000 locations within the volume of the phantom, essentially replacing a very high-resolution conventional grid or fiducial array phantom containing 11000 points. This greatly reduces cost, weight, and image processing and fiducial centroid detection time in automated software relative to conventional grid phantoms. Compared to a small fiducial array phantom that requires multiple time-consuming scan acquisitions at various locations and extended workflow (Schüler et al, 2020), or multiple slab 2D array phantoms with mechanical inaccuracies that only sample in seven single axial planes (Ranta et al, 2019), the MRID^{3D} phantom minimizes scan time with a single 5-minute

3D acquisition and simple workflow to achieve large FOV analysis of a high resolution true 3D Distortion Vector Field.

4.1. Spherical Harmonic Coefficient Output

Spherical Harmonic Coefficients (SHC) are useful in the correction of GNL, with the major MR vendors providing theoretically derived SHC for GNL correction. SHC are of interest to investigators improving DWI techniques through better Apparent Diffusion Coefficient (ADC) calibration, as ADC is known to be sensitive to GNL. The ability to acquire SHC in-situ empirically with a phantom has some advantages over theoretical SHC as in-situ measurements can consider subtle differences in manufacturing and installation (gradient coil cross talk, gradient coil system manufacturing tolerances and gradient coil misalignment errors etc.). The Harmonic Analysis method as employed in MRID^{3D} is ideally suited to measuring in-situ SHC output and represents for the first time a commercially available tool that is faster and easier to use than more laborious magnetic camera methods that require several hours of precise experimental set-up, data acquisition, data entry and analysis to arrive at a set of SHCs.

4.2. MRID^{3D} Phantom Construction

The MRID^{3D} phantom is constructed using two concentric acrylic cylinder tubes with a mineral oil filled gap between the two tubes, and two end plates with a similar mineral oil filled gap to form a complete enclosure. The resulting structure is mechanically robust and amenable for site-to-site shipping and multi-centre comparisons or commissioning. Mineral oil is used as it does not interact with acrylic (no swelling), has a low dielectric constant to avoid dielectric resonance effects at 3T, and provides a good susceptibility match to acrylic. Acrylic walls that separate air from the mineral oil MRI contrast media are designed to meet or exceed 6mm in thickness to reduce phantom susceptibility distortion.

Over 1500 small cylindrical blind holes are milled sufficiently deep into the outer surface of the inner cylinder and provide the necessary mineral oil filled fiducials. The net result is a large FOV phantom that weighs 21 kg with a hollow 25-liter air filled center, compared to an equivalent grid phantom that would weigh approximately 46 kg. Internal to the MRID^{3D} phantom is a mineral oil filled X, Y, Z cuboid with isocenter channel indicators to provide MRI signal at magnet isocenter for auto-prescanning, as well as features that are used by the automated software for orientation and twist correction information. Twist correction algorithms account for phantom misalignment due to end user positioning error, laser alignment system calibration errors, and patient table roll, pitch or yaw. In an experimental set-up with intentional twist, the MRID3D software accurately reports phantom twist, as well as laser system

calibration errors (1-degree twist in Y-axis (MR DICOM, Yaw) and a 4.5mm laser offset in Z due to laser miscalibration). On this MR system, a systemic 0.55-degree twist around the Z-axis (MR DICOM, Roll) is observed, likely due to mechanical level tolerances.

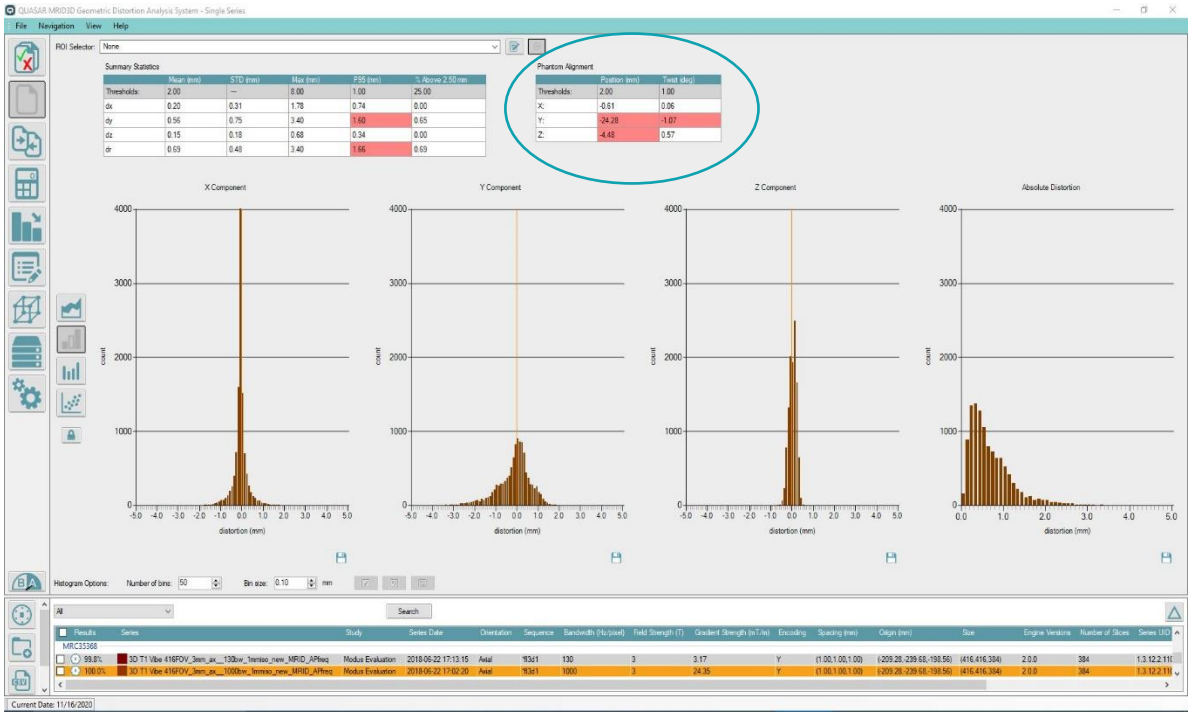

Figure 10. Patient table Roll, Pitch, and Yaw and Laser Alignment Errors relative to DICOM coordinates can be measured with MRID3D

A 6-axis CNC milling machine is used to mill fiducials in the MRID[3D] acrylic material. A 0.05 mm average manufacturing tolerance as measured with Mitutoyo Coordinate Measurement Machine Models CRTA-S9168 and CRTA-S574, calibrated to ISO/IEC 17025:2005 General Requirements for the Competence of Testing and Calibration Laboratories, has been verified.

Modus QA patents US10,180,484 (2017) and US10,310,048 (2019) describe the addition of thermal expansion chambers to MRID[3D] to provide compensation for thermal expansion of MR contrast liquid. Highly elastic fluorosilicone rubber tubes and membranes are added to the three oil filled reservoirs in MRID[3D] to provide geometric stability of the phantom structure.

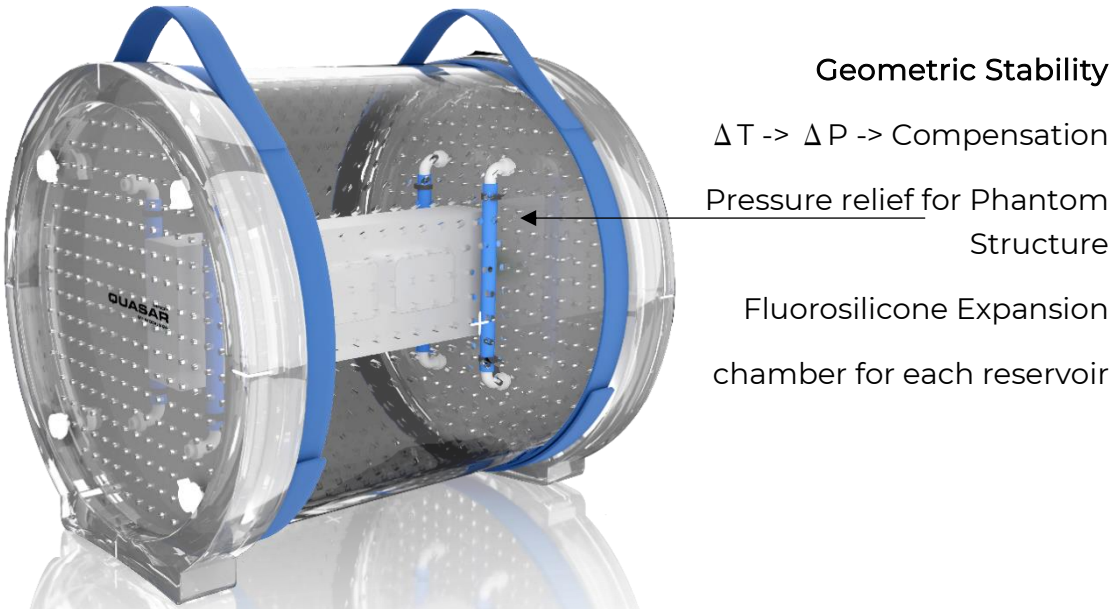

Figure 11. Temperature and pressure compensated phantom design – Modus QA MRID3D

FEM techniques have been implemented in the MRID^{3D} analysis software to further reduce phantom susceptibility distortion, with residual errors reported below 0.05mm in B_0 measurements in the non-frequency encode directions from 0.35T to 3.0T. As noted previously in (Baldwin *et al.*, 2007), scanning an object twice with opposing polarity in the frequency encode direction permits the separation of B_0 and Gradient Non-Linearity (GNL) distortion. Acquiring the two scans of the MRID^{3D} phantom and performing a scalar mathematical operation with the MRID^{3D} analysis software permits separating B_0 and GNL distortions. In theory, B_0 distortion in the non-frequency encode directions should be zero, but in practice some residual errors will remain.

Error estimation of the MRID3D Harmonic Analysis Boundary Phantom can be determined by acquiring two scans utilizing the reverse read out polarity method to separate B_0 and GNL(Baldwin et al 2007) and noting the residual B_0 distortion in the non-readout directions (0.03 mm in X and 0.02mm in Z below). Residual B_0 errors in the non-readout directions include the following:

- Gradient coil cross-talk
- Variance in vendor spherical harmonic correction
- Variance in gradient coil manufacturing
- Phantom manufacturing tolerance
- Partial volume effects on software twist correction

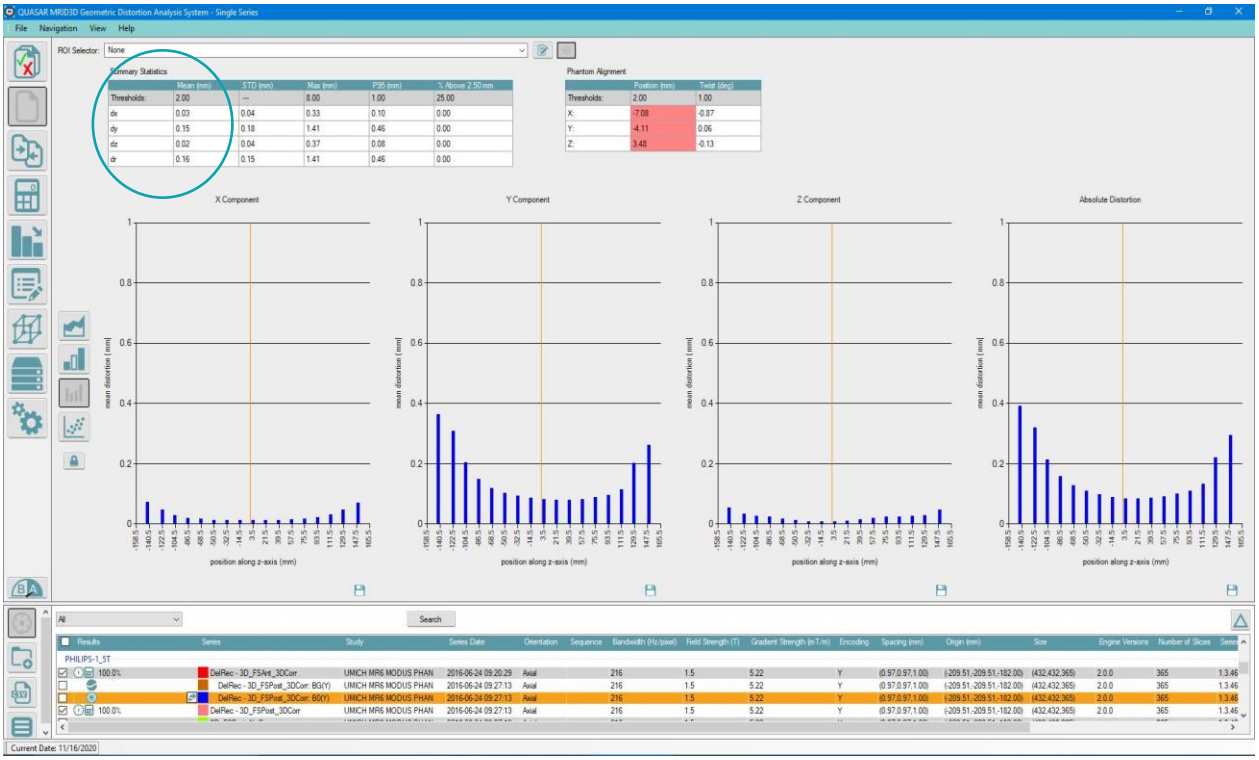

Figure 12. B0 Distortion in Y Frequency Encode Direction: distortion in X and Z are in theory zero but finite in practice

4.3. MRI Geometric Distortion in Gradient Recalled Echo Sequences Versus Spin Echo Sequences

Geometric distortion is noted as dependent on sequence type (Weygand *et al.*, 2016). A Spin Echo (SE) is produced by pairs of radiofrequency (RF) pulses, whereas a Gradient Recalled Echo (GRE) is produced by a single RF pulse in conjunction with a gradient reversal. In GRE imaging, the gradient reversal refocuses only those spins that have been dephased by action of the gradient itself. Phase shifts resulting from magnetic field inhomogeneities, static tissue susceptibility gradients, or chemical shifts are not cancelled at the center of the GRE as they are in SE sequences (Markl and Leupold, 2012). In modern 3D large FOV MRgRT Imaging applications on current MR-SIM and MR-Linac systems with low GNL and low B_0 distortion, GRE sequences are selected with higher bandwidths to mitigate distortion due to inhomogeneity, rendering the difference in distortion between practical, fast 3D GRE and SE sequences to negligible levels. A comparison of 1.5T 3D GRE and TSE sequences yield similar 3D distortion results over a large 35 cm FOV.

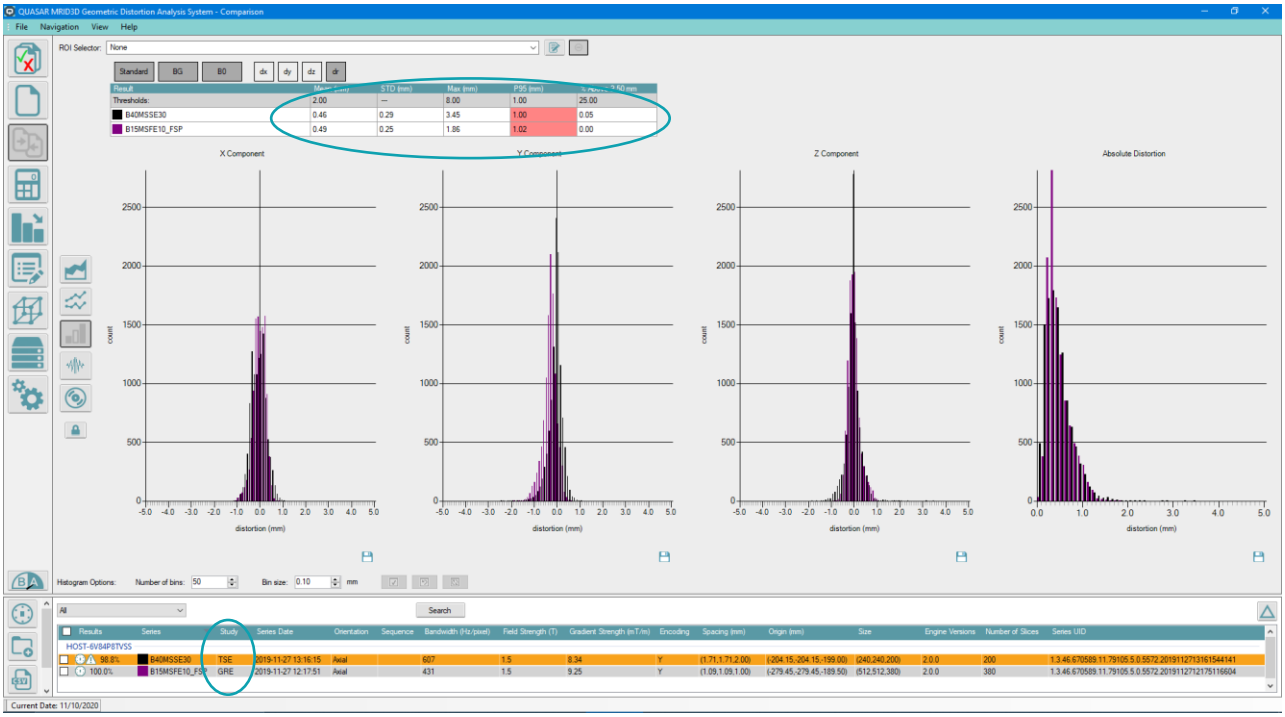

Figure 13. 3D GRE versus TSE Sequence yield very similar distortion results over a 35 cm FOV at 1.5T

5. Conclusion

A list of the factors previously noted that one must address to minimize error sources associated with geometric distortion QA phantom designs is summarized below. Note that these recommendations apply to all phantom types: grid, paint ball, boundary (Harmonic Analysis Method Based Geometric Distortion QA Phantom Design for Submillimeter Accuracy, Oral Scientific Presentation - MRinRT Toronto 2019; Rapid-fire Session: QA for MRI—guided radiotherapy).

- Compensate for thermal expansion of MR contrast liquid
- Use susceptibility matched plastic and MR contrast liquid
- Use thick material walls to separate air/material interface from fiducials, reduce phantom induced susceptibility distortion
- Use FEM techniques to further reduce residual phantom susceptibility distortion
- Use mineral oil for MR contrast media: plastic may absorb water and swell; water exhibits dielectric resonance effects at 3T
- Use a manufacturing method with tolerance below 0.1 mm (for 1 mm cubic voxels) and verify!

- Use automated software w/heuristics and phantom design elements to account for phantom/patient table misalignment and obtain robust landmark fiducial registration under conditions of high distortion

The above recommendations have been included in the updated industry standards listed below and implemented in the Modus QA MRID^{3D} phantom using the Harmonic Analysis method to demonstrate an estimated error of < 0.1 mm from 0.35T to 3T.

National Electrical Manufacturers Association - Medical Imaging Technology Alliance - NEMA MITA MS-12 2016 - *Quantification and Mapping of Geometric Distortion for Special Applications.*

International Electrotechnical Commission - IEC 62464-1 2018 *MAGNETIC RESONANCE EQUIPMENT FOR MEDICAL IMAGING – Part 1: Determination of essential image quality parameters*

NEMA MITA MS-12 2016 and IEC 62464-1 2018 Standards Technical Review and Maintenance Team Members: FDA, CFDA, Philips, Siemens, GE, Canon, Esaote, MR:Comp, Modus QA

Modus QA MRID^{3D} – a lighter, faster, large FOV Geometric Distortion Phantom using the Harmonic Analysis Method to set the standard for sub-millimeter accuracy and precision*.

**Phantom FEM-based Susceptibility Correction now available in MRID^{3D} v2.0.0, also including Spherical Harmonic Coefficient Output for DWI/GNL correction verification and ADC calibration validation.*

Sources and References

Figure Sources

Figure 1, 2, 7: Courtesy of Dr. Eric Paulson, Dept. of Radiology and Biophysics, Medical College of Wisconsin

Figure 6, 7: Courtesy of Dr. Teodor Stanescu, Radiation Medicine Program, Princess Margaret Cancer Centre

Figure 3, 4, 5, 8, 7, 9, 10, 11, 12, 13: Modus QA, MRID^{3D}, Software v2.0

References

Baldwin L N, Wachowicz K, Thomas S D, Rivest R and Fallone B G 2007 Characterization, prediction, and correction of geometric distortion in MR images *Medical Physics* **34** 388-99

Gach H M 2020 Technical Note: T1 and T2 and complex permittivities of mineral oil, silicone oil, and glycerol at 0.35, 1.5, and 3 T *Medical Physics* **46** 1785-92

Markl M and Leupold J 2012 Gradient echo imaging *Journal of Magnetic Resonance Imaging* **35** 1274-89

Ranta I, Kemppainen R, Keyriläinen J, Suilamo S, Heikkinen S, Kapanen M, Saunavaara J 2019 Quality assurance measurements of geometric accuracy for magnetic resonance imaging-based radiotherapy treatment planning *Physica Medica* **62** 47-52

Schenck J F 1996 The role of magnetic susceptibility in magnetic resonance imaging: MRI magnetic compatibility of the first and second kinds *Medical Physics* **23** 815-50

Schüler e, Mallozzi R, Levy J, Hristov D 2020 Technical Note: Extended field-of-view (FOV) MRI distortion

determination through multi-positional phantom imaging *J Appl Clin Med Phys* 1-11

Stanescu T and Jaffray D 2016 Management of MRI Spatial Accuracy for Radiation Therapy *MReadings: MR in RT* **2** 58-61

Stanescu T, Wachowicz K and Jaffray D A 2012 Characterization of tissue magnetic susceptibility-induced distortions for MRIgRT *Medical Physics* **39** 7185-93

Tadic T, Jaffray D A and Stanescu T 2014 Harmonic analysis for the characterization and correction of geometric distortion in MRI *Medical Physics* **41** 112303

Tijssen R H N, Vos R, Philippens M E P, van Lier A, Raaymakers B and van den Berg C 2019 Online Geometric Fidelity Inspection for MR-Guided Treatments on 1.5 T MRI-Linac: Visualizing the Cumulative Effect of Gradient Errors and Patient Specific Susceptibilities. In: *7th MRinRT Symposium,* (Toronto, Canada)

Wapler M C, Leupold J, Dragonu I, von Elverfeld D, Zaitsev M and Wallrabe U 2014 Magnetic properties of materials for MR engineering, micro-MR and beyond *Journal of Magnetic Resonance* **242** 233-42

Weygand J, Fuller C D, Ibbott G S, Mohamed A S R, Ding Y, Yang J, Hwang K-P and Wang J 2016 Spatial Precision in Magnetic Resonance Imaging–Guided Radiation Therapy: The Role of Geometric Distortion *International Journal of Radiation Oncology*Biology*Physics* **95** 1304-16

US Patent 9,857,443 B2 Tadic et al., Method and apparatus for the measurement, characterization and correction of geometric distortions in magnetic resonance imaging

US Patent 10,082,550 B2 Tadic et al., Method and apparatus for the measurement, characterization and correction of geometric distortions in magnetic resonance imaging: Continuation of US Patent 9,857,443 B2

US Patent 10,180,484 B2 Barberi et al., MRI quality assurance device

US Patent 10,310,048 B2 Barberi et al., MRI quality assurance device: Continuation of US Patent 10,180,484 B2

